NUREG/CR-0767
ORNL/NUREG-57

Application of Static and Dynamic Crack Arrest Theory to Thermal Shock Experiment TSE-4

R. D. Cheverton
S. K. Iskander

~~507 339~~

Prepared for the U.S. Nuclear Regulatory Commission
Office of Nuclear Regulatory Research
Under Interagency Agreements DOE 40-551-75 and 40-552-75

120555008386 2 ANRF
US NRC
SECY PUBLIC DOCUMENT ROOM
BRANCH CHIEF
WASHINGTON DC 20555

OAK RIDGE NATIONAL LABORATORY
OPERATED BY UNION CARBIDE CORPORATION · FOR THE DEPARTMENT OF ENERGY

508 001

7906070781

Printed in the United States of America. Available from
National Technical Information Service
U.S. Department of Commerce
5285 Port Royal Road, Springfield, Virginia 22161

This report was prepared as an account of work sponsored by an agency of the United States Government. Neither the United States Government nor any agency thereof, nor any of their employees, contractors, subcontractors, or their employees, makes any warranty, express or implied, nor assumes any legal liability or responsibility for any third party's use or the results of such use of any information, apparatus, product or process disclosed in this report, nor represents that its use by such third party would not infringe privately owned rights.

508 002
~~507 340~~

NUREG/CR-0767
ORNL/NUREG-57
Dist. Category RF

Contract No. W-7405-eng-26

Engineering Technology Division

APPLICATION OF STATIC AND DYNAMIC CRACK ARREST THEORY TO THERMAL SHOCK EXPERIMENT TSE-4

R. D. Cheverton
S. K. Iskander

Manuscript Completed — May 10, 1979
Date Published — June 1979

Prepared for the
U.S. Nuclear Regulatory Commission
Office of Nuclear Regulatory Research
Washington, D.C. 20555
Under Interagency Agreements DOE 40-551-75 and 40-552-75

NRC FIN No. B0119

Prepared by the
OAK RIDGE NATIONAL LABORATORY
Oak Ridge, Tennessee 37830
operated by
UNION CARBIDE CORPORATION
for the
DEPARTMENT OF ENERGY

508 003

~~507 341~~

CONTENTS

508 004

FOREWORD

The work reported here was performed at Oak Ridge National Laboratory (ORNL) under sponsorship of the U.S. Nuclear Regulatory Commission's (NRC's) Heavy-Section Steel Technology (HSST) Program, which is directed by ORNL. The program is conducted as part of the ORNL Pressure Vessel Technology Program, of which G. D. Whitman is manager. The NRC manager is C. Z. Serpan.

This report is designated Heavy-Section Steel Technology Program Technical Report No. 52. Prior reports in this series are listed below.

1. S. Yukawa, *Evaluation of Periodic Proof Testing and Warm Prestressing Procedures for Nuclear Reactor Vessels*, HSSTP-TR-1, General Electric Company, Schenectady, N.Y. (July 1, 1969).

2. L. W. Loechel, *The Effect of Section Size on the Transition Temperature in Steel*, MCR-69-189, Martin Marietta Corporation, Denver, Col. (Nov. 20, 1969).

3. P. N. Randall, *Gross Strain Measure of Fracture Toughness of Steels*, HSSTP-TR-3, TRW Systems Group, Redondo Beach, Calif. (Nov. 1, 1969).

4. C. Visser, S. E. Gabrielse, and W. VanBuren, *A Two-Dimensional Elastic-Plastic Analysis of Fracture Test Specimens*, WCAP-7368, Westinghouse Electric Corporation, PWR Systems Division, Pittsburgh, Pa. (October 1969).

5. T. R. Mager, F. O. Thomas, and W. S. Hazelton, *Evaluation by Linear Elastic Fracture Mechanics of Radiation Damage to Pressure Vessel Steels*, WCAP-7328 (Rev.), Westinghouse Electric Corporation, PWR Systems Division, Pittsburgh, Pa. (October 1969).

6. W. O. Shabbits, W. H. Pryle, and E. T. Wessel, *Heavy-Section Fracture Toughness Properties of A533 Grade B Class 1 Steel Plate and Submerged Arc Weldment*, WCAP-7414, Westinghouse Electric Corporation, PWR Systems Division, Pittsburgh, Pa. (December 1969).

7. F. J. Loss, *Dynamic Tear Test Investigations of the Fracture Toughness of Thick-Section Steel*, NRL-7056, U.S. Naval Research Laboratory, Washington, D.C. (May 14, 1970).

8. P. B. Crosley and E. J. Ripling, *Crack Arrest Fracture Toughness of A533 Grade B Class 1 Pressure Vessel Steel*, HSSTP-TR-8, Materials Research Laboratory, Inc., Glenwood, Ill. (March 1970).

9. T. R. Mager, *Post-Irradiation Testing of 2 T Compact Tension Specimens*, WCAP-7561, Westinghouse Electric Corporation, PWR Systems Division, Pittsburgh, Pa. (August 1970).

10. T. R. Mager, *Fracture Toughness Characterization Study of A 533, Grade B, Class 1 Steel*, WCAP-7578, Westinghouse Electric Corporation, PWR Systems Division, Pittsburgh, Pa. (October 1970).

11. T. R. Mager, *Notch Preparation in Compact Tension Specimens*, WCAP-7579, Westinghouse Electric Corporation, PWR Systems Division, Pittsburgh, Pa. (November 1970).

12. N. Levy and P. V. Marcal, *Three-Dimensional Elastic-Plastic Stress and Strain Analysis for Fracture Mechanics, Phase I: Simple Flawed Specimens*, HSSTP-TR-12, Brown University, Providence, R.I. (December 1970).

13. W. O. Shabbits, *Dynamic Fracture Toughness Properties of Heavy Section A533 Grade B, Class 1 Steel Plate*, WCAP-7623, Westinghouse Electric Corporation, PWR Systems Division, Pittsburgh, Pa. (December 1970).

14. P. N. Randall, *Gross Strain Crack Tolerance of A533-B Steel*, HSSTP-TR-14, TRW Systems Group, Redondo Beach, Calif. (May 1, 1971).

15. H. T. Corten and R. H. Sailors, *Relationship between Material Fracture Toughness Using Fracture Mechanics and Transition Temperature Tests*, T&AM Report 346, University of Illinois, Urbana, Ill. (Aug. 1, 1971).

16. T. R. Mager and V. J. McLoughlin, *The Effect of an Environment of High Temperature Primary Grade Nuclear Reactor Water and the Fatigue Crack Growth Characteristics of A533 Grade B Class 1 Plate and Weldment Material*, WCAP-7776, Westinghouse Electric Corporation, PWR Systems Division, Pittsburgh, Pa. (October 1971).

17. N. Levy and P. V. Marcal, *Three-Dimensional Elastic-Plastic Stress and Strain Analysis for Fracture Mechanics, Phase II: Improved Modeling*, HSSTP-TR-17, Brown University, Providence, R.I. (November 1971).

18. S. C. Grigory, *Six-Inch-Thick Flawed Tensile Tests, First Technical Summary Report, Longitudinal Specimens 1 through 7*, HSSTP-TR-18, Southwest Research Institute, San Antonio, Tex. (June 1972).

19. P. N. Randall, *Effects of Strain Gradients on the Gross Strain Crack Tolerance of A533-B Steel*, HSSTP-TR-19, TRW Systems Group, Redondo Beach, Calif. (May 1, 1972).

20. S. C. Grigory, *Tests of Six-Inch-Thick Flawed Tensile Specimens, Second Technical Summary Report, Transverse Specimens Numbers 8 through 10, Welded Specimens Numbers 11 through 13*, HSSTP-TR-20, Southwest Research Institute, San Antonio, Tex. (June 1972).

21. L. A. James and J. A. Williams, *Heavy-Section Steel Technology Program Technical Report No. 21, The Effect of Temperature and Neutron Irradiation upon the Fatigue-Crack Propagation Behavior of ASTM A533, Grade B, Class 1 Steel*, HEDL-TME-72-132, Hanford Engineering Development Laboratory, Richland, Wash. (September 1972).

508 09

22. S. C. Grigory, *Tests of Six-Inch-Thick Flawed Tensile Specimens, Third Technical Summary Report, Longitudinal Specimens Numbers 14 through 16, Unflawed Specimen Number 17*, HSSTP-TR-22, Southwest Research Institute, San Antonio, Tex. (October 1972).

23. S. C. Grigory, *Tests of Six-Inch-Thick Flawed Tensile Specimens, Fourth Technical Summary Report, Tests of One-Inch-Thick Flawed Tensile Specimens for Size Effect Evaluation*, HSSTP-TR-23, Southwest Research Institute, San Antonio, Tex. (June 1973).

24. S. P. Ying and S. C. Grigory, *Tests of Six-Inch-Thick Tensile Specimens, Fifth Technical Summary Report, Acoustic Emission Monitoring of One-Inch and Six-Inch-Thick Tensile Specimens*, HSSTP-TR-24, Southwest Research Institute, San Antonio, Tex. (November 1972).

25. R. W. Derby et al., *Test of 6-Inch-Thick Pressure Vessels, Series 1: Intermediate Test Vessels V-1 and V-2*, ORNL-4895, Oak Ridge National Laboratory, Oak Ridge, Tenn. (February 1974).

26. W. J. Stelzman and R. G. Berggren, *Radiation Strengthening and Embrittlement in Heavy-Section Plates and Welds*, ORNL-4871, Oak Ridge National Laboratory, Oak Ridge, Tenn. (June 1973).

27. P. B. Crosley and E. J. Ripling, *Crack Arrest in an Increasing K-Field*, HSSTP-TR-27, Materials Research Laboratory, Glenwood, Ill. (January 1973).

28. P. V. Marcal, P. M. Stuart, and R. S. Bettes, *Elastic-Plastic Behavior of a Longitudinal and Semi-Elliptical Crack in a Thick Pressure Vessel*, Brown University, Providence, R.I. (June 1973).

29. W. J. Stelzman, *Characterization of HSST Plate 02* (in preparation).

30. D. A. Canonico, *Characterization of Heavy-Section Weldments in Pressure Vessel Steels* (in preparation).

31. J. A. Williams, *The Irradiation and Temperature Dependence of Tensile and Fracture Properties of ASTM A533, Grade B, Class 1 Steel Plate and Weldment*, HEDL-TME 73-75, Hanford Engineering Development Laboratory, Richland, Wash. (August 1973).

32. J. M. Steichen and J. A. Williams, *High Strain Rate Tensile Properties of Irradiated ASTM A533, Grade B, Class 1 Pressure Vessel Steel*, Hanford Engineering Development Laboratory, Richland, Wash. (July 1973).

33. P. C. Riccardella and J. L. Swedlow, *A Combined Analytical-Experimental Fracture Study*, WCAP-8224, Westinghouse Electric Corporation, PWR Systems Division, Pittsburgh, Pa. (October 1973).

34. R. J. Podlasek and R. J. Eiber, *Final Report on Investigation of Mode III Crack Extension in Reactor Piping*, Battelle Columbus Laboratories, Columbus, Ohio (May 1974).

35. T. R. Mager et al., *Interim Report on the Effect of Low Frequencies on the Fatigue Crack Growth Characteristics of A533, Grade B, Class 1 Plate in an Environment of High-Temperature Primary Grade Nuclear Reactor Water*, WCAP-8256, Westinghouse Electric Corporation, Pittsburgh, Pa. (December 1973).

36. J. A. Williams, *The Irradiated Fracture Toughness of ASTM A533, Grade B, Class 1 Steel Measured with a Four-Inch-Thick Compact Tension Specimen*, HEDL-TME 75-10, Hanford Engineering Development Laboratory, Richland, Wash. (January 1975).

37. R. H. Bryan et al., *Test of 6-Inch-Thick Pressure Vessels, Series 2: Intermediate Test Vessels V-3, V-4, and V-6*, ORNL-5059, Oak Ridge National Laboratory, Oak Ridge, Tenn. (November 1975).

38. T. R. Mager, S. E. Yanichko, and L. R. Singer, *Fracture Toughness Characterization of HSST Intermediate Pressure Vessel Material*, WCAP-8456, Westinghouse Electric Corporation, Pittsburgh, Pa. (December 1974).

39. J. G. Merkle, G. D. Whitman, and R. H. Bryan, *An Evaluation of the HSST Program Intermediate Pressure Vessel Tests in Terms of Light-Water Reactor Pressure Vessel Safety*, ORNL/TM-5090, Oak Ridge National Laboratory, Oak Ridge, Tenn. (November 1975).

40. J. G. Merkle et al., *Test of 6-Inch-Thick Pressure Vessels. Series 3: Intermediate Test Vessel V-7*, ORNL/NUREG-1, Oak Ridge National Laboratory, Oak Ridge, Tenn. (August 1976).

41. J. A. Davidson et al., *The Irradiated Dynamic Fracture Toughness of ASTM A533, Grade B, Class 1 Steel Plate and Submerged Arc Weldment*, WCAP-8775, Westinghouse Electric Corporation, Pittsburgh, Pa. (October 1976).

42. R. D. Cheverton, *Pressure Vessel Fracture Studies Pertaining to a PWR LOCA-ECC Thermal Shock: Experiments TSE-1 and TSE-2*, ORNL/NUREG/TM-31, Oak Ridge National Laboratory, Oak Ridge, Tenn. (September 1976).

43. J. G. Merkle et al., *Test of 6-Inch-Thick Pressure Vessels. Series 4: Intermediate Test Vessels V-5 and V-9 with Inside Nozzle Cracks*, ORNL/NUREG-7, Oak Ridge National Laboratory, Oak Ridge, Tenn. (August 1977).

44. J. A. Williams, *The Ductile Fracture Toughness of Heavy-Section Steel Plate*, Hanford Engineering Development Laboratory, Richland, Wash. (in preparation).

45. R. H. Bryan, J. G. Merkle, and G. C. Smith, *Test of 6-Inch-Thick Pressure Vessels. Series 3: Intermediate Test Vessel V-7A under Sustained Loading*, ORNL/NUREG-9, Oak Ridge National Laboratory, Oak Ridge, Tenn. (February 1978).

508 008

46. R. D. Cheverton and S. E. Bolt, *Pressure Vessel Fracture Studies Pertaining to a PWR LOCA-ECC Thermal Shock: Experiments TSE-3 and TSE-4, and Update of TSE-1 and TSE-2 Analysis*, ORNL/NUREG-22, Oak Ridge National Laboratory, Oak Ridge, Tenn. (December 1977).

47. D. A. Canonico, *Significance of Reheat Cracks to the Integrity of Pressure Vessels for Light-Water Reactors*, ORNL/NUREG-15, Oak Ridge National Laboratory, Oak Ridge, Tenn. (July 1977).

48. G. C. Smith and P. P. Holz, *Repair Weld Induced Residual Stresses in Thick-Walled Steel Pressure Vessels*, ORNL/NUREG/TM-153, Oak Ridge National Laboratory, Oak Ridge, Tenn. (in preparation).

49. P. P. Holz and S. W. Wismer, *Half-Bead (Temper) Repair Welding for HSST Vessels*, ORNL/NUREG/TM-177, Oak Ridge National Laboratory, Oak Ridge, Tenn. (in preparation).

50. G. C. Smith, P. P. Holz, and W. J. Stelzman, *Crack Extension and Arrest Tests of Axially Flawed Steel Model Pressure Vessels*, ORNL/NUREG/TM-196, Oak Ridge National Laboratory, Oak Ridge, Tenn. (in preparation).

51. R. H. Bryan et al., *Test of 6-in.-Thick Pressure Vessels. Series 3: Intermediate Test Vessel V-7B*, ORNL/NUREG/38, Oak Ridge National Laboratory, Oak Ridge, Tenn. (in preparation).

52. R. D. Cheverton, S. K. Iskander, and S. E. Bolt, *Applicability of LEFM to the Analysis of PWR Vessels Under LOCA-ECC Thermal Shock Conditions*, ORNL/NUREG-40, Oak Ridge National Laboratory, Oak Ridge, Tenn. (October 1978).

53. R. H. Bryan et al., *Test of 6-in.-Thick Pressure Vessels. Series 3: Intermediate Test Vessel V-8*, NUREG/CR-0675 (ORNL/NUREG-58), Oak Ridge National Laboratory, Oak Ridge, Tenn. (in preparation).

Copies of these reports may be obtained from the Laboratory Records Department, Oak Ridge National Laboratory, P.O. Box X, Oak Ridge, Tenn. 37830.

NOMENCLATURE

a	Depth of flaw
$\dot{a}$	Crack velocity
a_c	Critical crack depth corresponding to a particular event or condition
w	Thickness of vessel w ıl
K_I	Mod I stress-intensity factor
K_{Ia}	K_I value at time of crack arrest, based on static calculation
K_{Ic}	Static fracture toughness
K_{ID}	Actual K_I value while crack is running
K_{Im}	Actual value of K_I at time of arrest (minimum value of K_{ID} that can sustain crack propagation)
K_Q	K_I value at initiation assuming a sharp crack

APPLICATION OF STATIC AND DYNAMIC CRACK ARREST THEORY TO THERMAL SHOCK EXPERIMENT TSE-4

R. D. Cheverton
S. K. Iskander

ABSTRACT

A dynamic method of analysis developed by Battelle Columbus Laboratory (BCL) for a crack run-arrest event was applied to Oak Ridge National Laboratory (ORNL) thermal shock experiment TSE-4, which was conducted on an A508 steel cylinder [530 mm OD × 150 mm wall × 910 mm long (21 in. × 6 in. × 36 in.)] with a quench-only heat treatment. In this experiment, a long axial flaw with an initial depth of 11 mm propagated in a single jump to a depth of 23 mm and arrested. The dynamic analysis indicated that dynamic effects for the 12-mm extension were essentially negligible; thus the statically calculated arrest toughness (K_{Ia}) was a good approximation of K_{Im}. This K_{Im} (K_{Ia}) value (127 MN $m^{-3/2}$) was 24% less than K_{Ic} at the same temperature (131°C). The K_{Im} value deduced from the dynamic analysis of TSE-4 was 124 MN $m^{-3/2}$, which is in good agreement with the statically calculated value of K_{Ia} at arrest (127 MN $m^{-3/2}$).

Researchers at BCL obtained several values of K_{ID} for the TSE-4-type material. However, data were insufficient for determining a laboratory value of K_{Im}, which could have been compared to the TSE-4 K_{Im} value. All values of K_{ID} obtained by BCL were greater than K_{Ic}.

1. INTRODUCTION

The Oak Ridge National Laboratory (ORNL) Heavy-Section Steel Technology (HSST) Thermal Shock Program was established to investigate means for predicting the fracture behavior of pressurized-water reactor (PWR) pressure vessels when subjected to severe thermal shock. The thermal-type loading could result from hypothetical loss-of-coolant or steam-line-break accidents, wherein relatively cool water passes over the inner surface of the hot pressure vessel wall. As shown in Fig. 1, for a typical double-ended-pipe-break LOCA-ECC,* this rapid quenching of the inner surface results in rather steep positive temperature gradients through the wall and thus high tensile stresses in the inner portion of the wall. The

*For brevity in this report, the loss-of-coolant accident followed by injection of emergency core coolant is referred to as LOCA-ECC.

ORNL DWG 79 4353 ETD

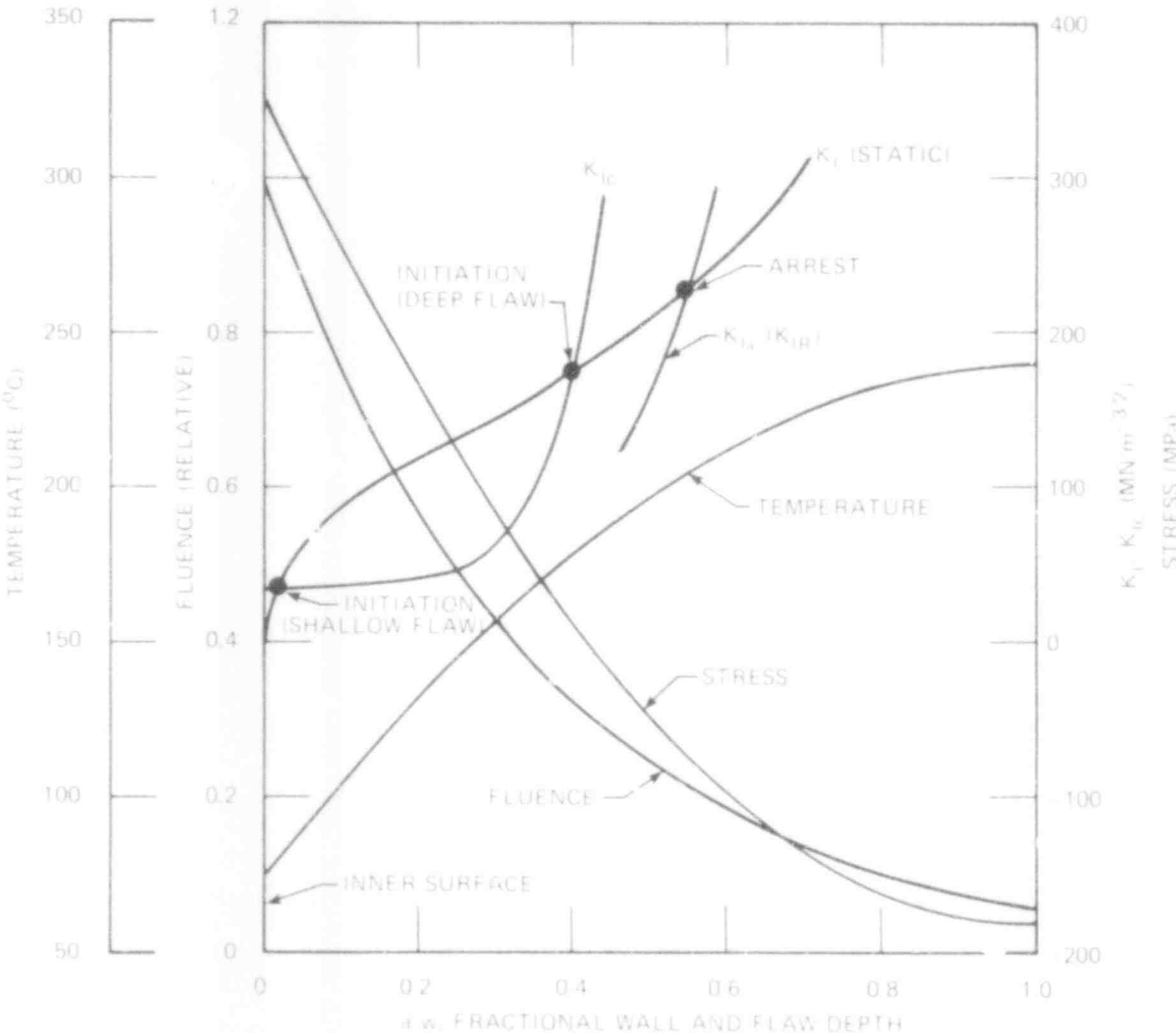

Fig. 1. Typical instantaneous temperature, stress, fluence, stress-intensity factor, and fracture and arrest toughness (high-copper material) for a PWR vessel subjecte to a LOCA-ECC thermal shock (maximum fluence = 4×10^{19} n/cm^2).

reduction in temperature and the high fast-neutron fluence that accumulates over many years of reactor operation tend to reduce the fracture toughness (K_{Ic}) of the vessel material. Because of the sensitivity of fracture toughness to temperature and fluence, the positive gradient in temperature, and the attenuation of the fluence, there is a net positive gradient in toughness in the vessel wall.

508 012

If there is a flaw on the inner surface of the vessel wall, the high, thermally induced tensile stress will result in an appreciable stress-intensity factor (K_I) at the tip of the flaw, as indicated in Fig. 1. The combined effect of high stress-intensity factor and low fracture toughness may result in propagation of the flaw. However, the steep positive gradient in toughness tends to provide a mechanism for arresting the crack.

The ORNL Thermal Shock Program included experiments in which rather large steel cylinders [530 mm OD × 150 mm wall × 910 mm long (21 in. × 6 in. × 36 in.)] (see Fig. 2) containing flaws on the inner surface were subjected to severe thermal shock, with the coolant applied to the inner surface. The experiments were designed so that both initiation and arrest of specially prepared flaws presumably would take place. Four experiments have been conducted and are discussed in detail elsewhere[1-3] with regard to test conditions and a static analysis of the da This report contains a review of the static analysis and a dynamic analysis of the run-arrest event in the fourth experiment (TSE-4), which was better suited than the others to such an analysis. TSE-4 provided the first opportunity to apply a dynamic method of analysis to a structure substantially larger than arrest-toughness-type laboratory specimens.

A dynamic method of analysis for describing run-arrest events[4,5] and a procedure for measuring crack-arrest toughness[6] have been under development at Battelle Columbus Laboratory (BCL) for some time, and, as mentioned above, ORNL has been conducting initiation-arrest experiments on large specimens. To take full advantage of these efforts, the Nuclear Regulatory Commission (NRC) established a cooperative program between the two laboratories. One of the objectives of the ongoing program is to compare arrest-toughness values measured in the laboratory under mechanical loading conditions with values deduced from experiments with much larger specimens under thermal shock loading conditions. Side grooves are used in the laboratory specimens in an attempt to cope with the size problem, but as Irwin[7] pointed out, "Use of deep face grooves to overcome testing problems in the high toughness range introduces serious questions as to the applicability of test results to natural cracks in heavy section structures."

Another objective of the program is to determine how accurately the BCL dynamic method of analysis can describe a run-arrest event in the

508 013

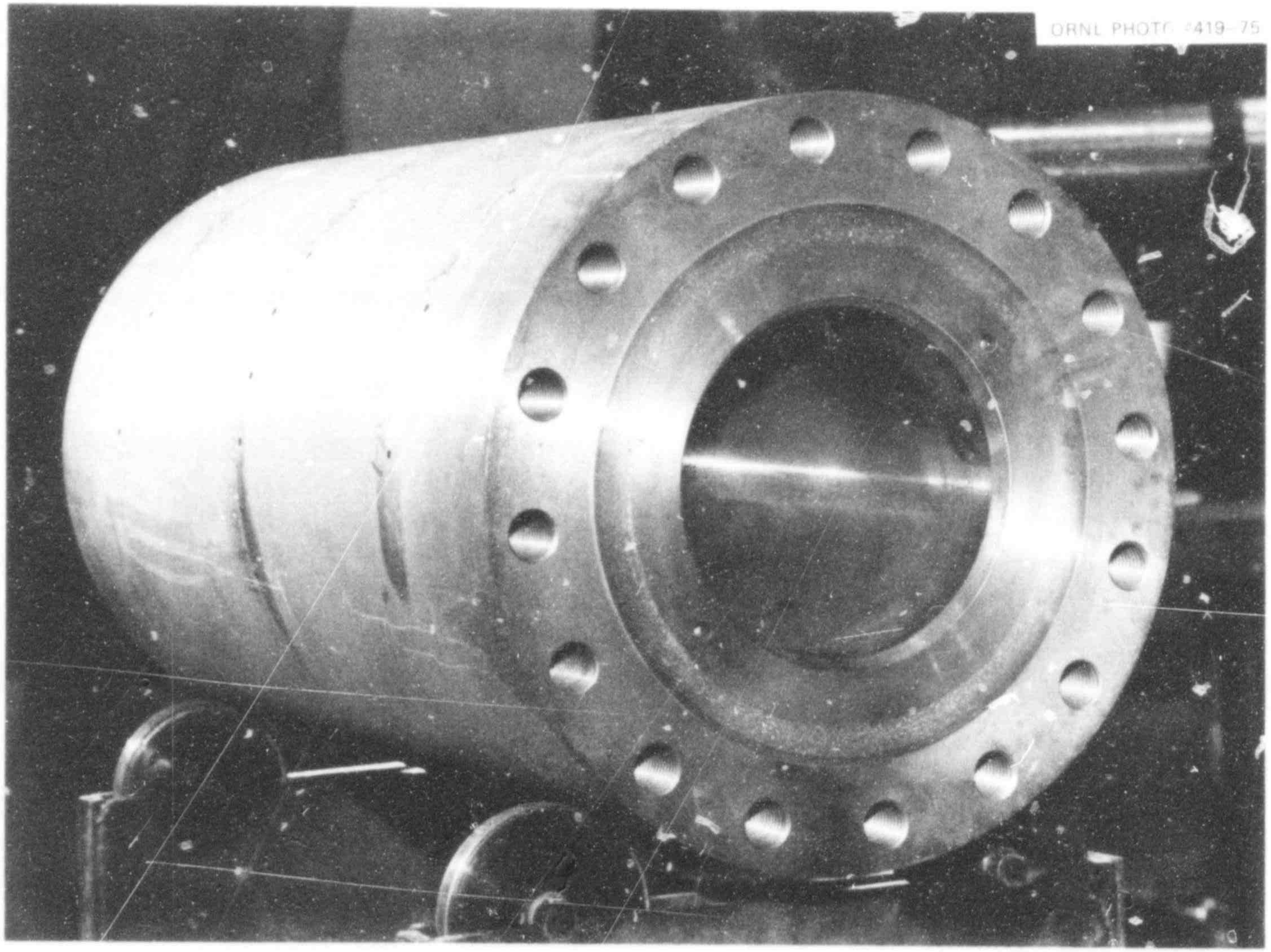

Fig. 2. One of two 533-mm-OD (21-in.) thermal shock test specimens.

large test cylinders using laboratory crack-arrest toughness data and the actual temperature gradients in the cylinder wall. Fulfillment of these objectives will help to establish the adequacy of the crack-arrest methodology for safety analysis and design purposes.

500 015 ~~14~~

2. THE BCL DYNAMIC METHOD OF ANALYSIS

Crack propagation (unstable) and arrest involve acceleration of material surrounding the crack; thus the run-arrest event is a dynamic one.[8-10] The magnitude of the dynamic effect relative to a static analysis of the event will vary depending on the size of the crack jump relative to a body dimension, such as the uncracked ligament in a pressure vessel wall or in a laboratory specimen used to measure arrest toughness.[11] If the crack jump is short enough, the dynamic effects will be negligible, and a static analysis will suffice. However, it seems that a dynamic analysis would be required to determine the extent of the dynamic effect in any particular structure.

The dynamic method of analysis being developed by BCL, which seeks to account for kinetic energy and inertia in the calculation of K_I, is described in detail in Ref. 4. Kalthoff et al.[11] have shown that, during the early portion of crack propagation, the actual K_I value tends to lag behind the statically calculated value, whereas, at later times and at arrest, the actual value of K_I is greater than the statically calculated value. This same trend is predicted with the BCL dynamic method of analysis.[4]

The actual instantaneous K_I value while the crack is running is referred to as K_{ID} and may be dependent on crack velocity ($\dot{a}$).[6,12] Presumably, there is a minimum value of K_{ID}, referred to as K_{Im}, below which crack propagation cannot be sustained; K_{Im} may correspond to a minimum value of $\dot{a}$ but not necessarily zero velocity. Possible K_{ID} vs $\dot{a}$ curves[6] are shown in Fig. 3. In Fig. 3(a), $K_{ID} > K_{Ic}$ for all values of $\dot{a}$ except at zero velocity, where $K_{Im} = K_{ID} \cong K_{Ic}$. This condition has been observed for a high-strength steel.[13] Figure 3(b) illustrates a case for which $K_{ID} < K_{Ic}$ for low velocities, and $K_{ID} > K_{Ic}$ for higher velocities. For this case, $K_{Im} < K_{Ic}$ and $(\dot{a})_{K_{Im}} > 0$.

The BCL analysis requires a description of the K_{ID} vs $\dot{a}$ and the K_{ID} vs temperature curves and also requires as input the value of K_I at the time of initiation. This latter value is referred to as K_Q and may or may not be equal to K_{Ic}, depending on whether the initial flaw is sharp or not; if the flaw is blunted, $K_Q > K_{Ic}$. During the dynamic calculation,

508 016

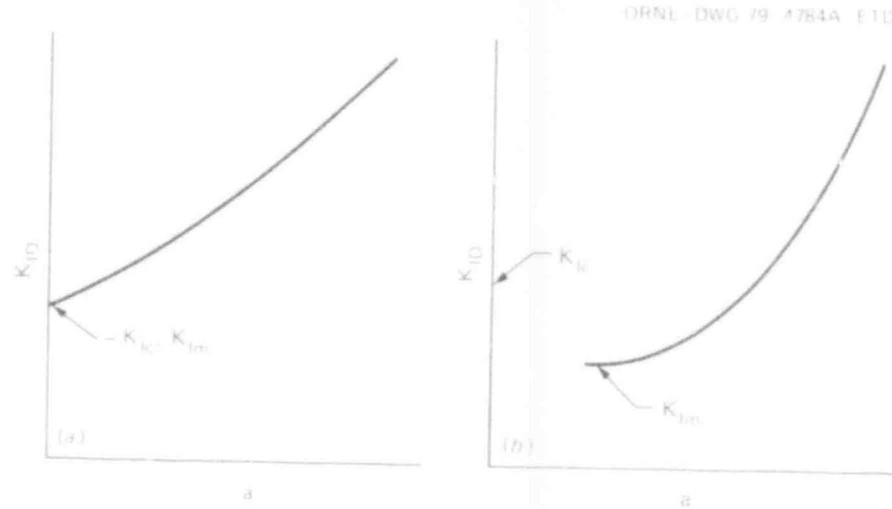

Fig. 3. Two possible types of K_{ID} vs $\dot{a}$ curves: (a) $K_{Im} = K_{Ic}$; (b) $K_{Im} < K_{Ic}$.

the K_I value is monitored; when K_I drops below K_{Im}, the crack is considered to be arrested.

3. MATERIAL PROPERTIES FOR TSE-4 TEST CYLINDER

Two test cylinders (TSV-1 and TSV-2) were used in the series of thermal shock experiments at ORNL, with TSV-2 being used for TSE-4. To simulate postulated PWR fracture conditions as closely as possible, the two test cylinders were fabricated from pressure-vessel grade A508 steel and were given a quench-only heat treatment. This treatment reduces toughness and increases yield strength relative to the standard quenched and tempered condition — changes which simulate irradiation effects to some extent.

Most of the material property data for TSV-1 and TSV-2 were obtained by ORNL, using prolongations of the two test cylinders; the data included tensile, Charpy-V, and static fracture toughness (precracked Charpy and compact-tension) data. A few material characterizations were conducted at BCL and were performed on material taken from TSV-1 after completion of the thermal shock experiments. These included static fracture toughness tests and crack-arrest toughness measurements. Most of the ORNL data are reported in Ref. 3, and all the toughness data are summarized in this report.

No systematic differences between the results for TSV-1 and TSV-2 or associated distances from the surfaces were apparent. The yield and ultimate strengths of the A508 material in the quench-only condition are nearly independent of temperature in the range −73 to 260°C, and have average values of 970 and 1170 MPa, respectively, which are quite high relative to values for the normal tempered condition. The static fracture toughness values, on the other hand, tend to be relatively low and are plotted in Fig. 4 for the measured temperature range of −196 to 149°C (−320 to 300°F). Also included in this figure are the K_{Ic} values measured by BCL and the single value of arrest-toughness determined by the ORNL static analysis of the arrest event in TSE-4.

Laboratory crack-arrest toughness measurements were performed by BCL on wedge-loaded duplex rectangular (DCB) specimens.[6] Two data sets were obtained at each of two temperatures (78 and 126°C), which correspond closely to the TSE-4 initiation and arrest temperatures. The measured K_{Ia} and K_{ID} values are shown in Table 1. As indicated in this table, only one value of K_{ID} and corresponding value of $\dot{a}$ are given for each specimen

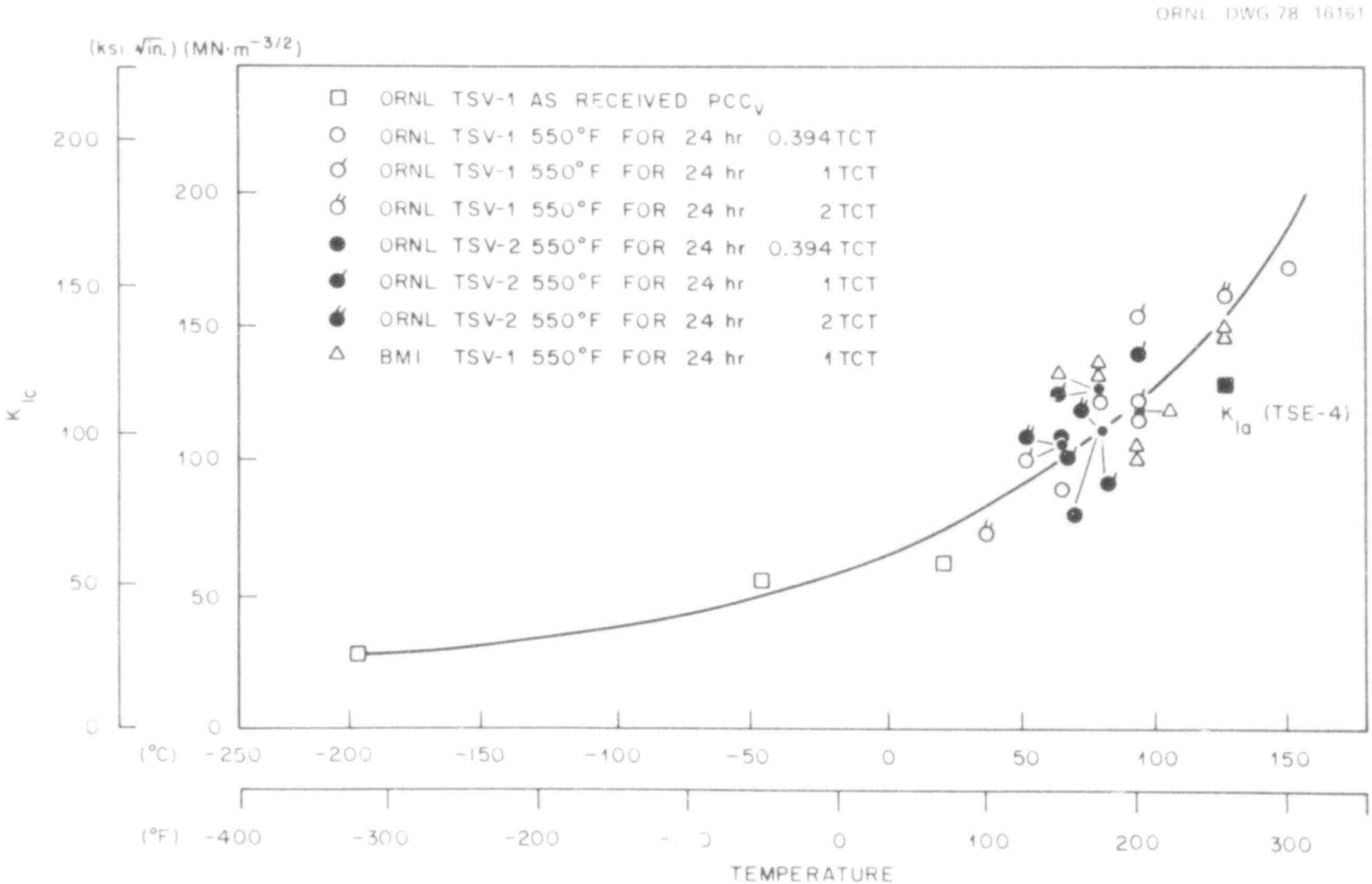

Fig. 4. K_{Ic} vs temperature for TSV-1 and TSV-2 material (A508 quench only).

Table 1. BCL crack-arrest toughness measurements for TSE-4

DCB specimen	Test temperature (°C)	K_{Ia} (MN m$^{-3/2}$)	K_{ID} (MN m$^{-3/2}$)	$\dot{a}$ (msec^{-1})
OR-5	126	122	172	670
OR-6	126	125	173	700
OR-7	78	106	157	780
OR-8	78	[illegible]	149	710

tested, although a range of velocities, and thus K_{ID} values, exists during the run event. For most of the crack time-of-flight, K_{ID} and $\dot{a}$ are nearly constant,[11] and these are the values reported. Data of this type are sufficient for determining K_{Im}, provided that enough data points are available for defining the minimum in the curve. In this particular case, two values of K_{ID} were not sufficient for determining K_{Im}.

The static fracture toughness values (K_{Ia}) reported by BCL were determined by means of a static analysis of K_I in accordance with a procedure proposed by Materials Research Laboratory,[14] and they effectively constitute the static K_I value at the time of arrest. As indicated in Sect. 2, K_{Ia} should be less than K_{Im}.

508 020

4. RESULTS OF TSE-4

A summary of test conditions for TSE-4 is presented in Table 2. Data retrieved from the experiment included the temperature distribution through the wall as a function of time and indications of crack initiation and arrest as detected by crack-opening-displacement gages and acoustic emission instrumentation. At the completion of the experiment, the temperature distributions were used as the thermal loadings for the calculation of the stress-intensity factors.

The TSE-4 test cylinder initially contained an 11-mm-deep axial crack that extended the full length of the cylinder. During the thermal transient, crack initiation and arrest took place along the entire crack front at 150 sec. Indications of the cracking are shown in Fig. 5, a photograph of the inner surface of TSV-2 following TSE-4, and in Fig. 6, which shows the fracture surfaces after removal from the cylinder.

The measured radial temperature profile, the calculated K_I distribution (assuming various crack depths), and the nominal K_{Ic} radial distribution (based on the K_{Ic} vs temperature curve in Fig. 4), all corresponding

Table 2. Test conditions and material properties for TSE-4

Test specimen dimensions, m (in.)	
OD	0.53 (21)
ID	0.24 (9.5)
Length	0.91 (36)
Test specimen material	A508, class 2
Heat treatment	Quench only from 871°C (1600°F)
Flaw	Long axial crack
Initial depth, mm (in.)	11 ± 1 (0.44 ± 0.03)
Final (arrested) depth, mm (in.)	23 ± 2 (0.91 ± 0.09)
Temperatures (initial), °C (°F)	
Wall	291 (555)
Sink	−25 (−13)
Coolant	40 wt % methyl alcohol, 60 wt % water

508 021

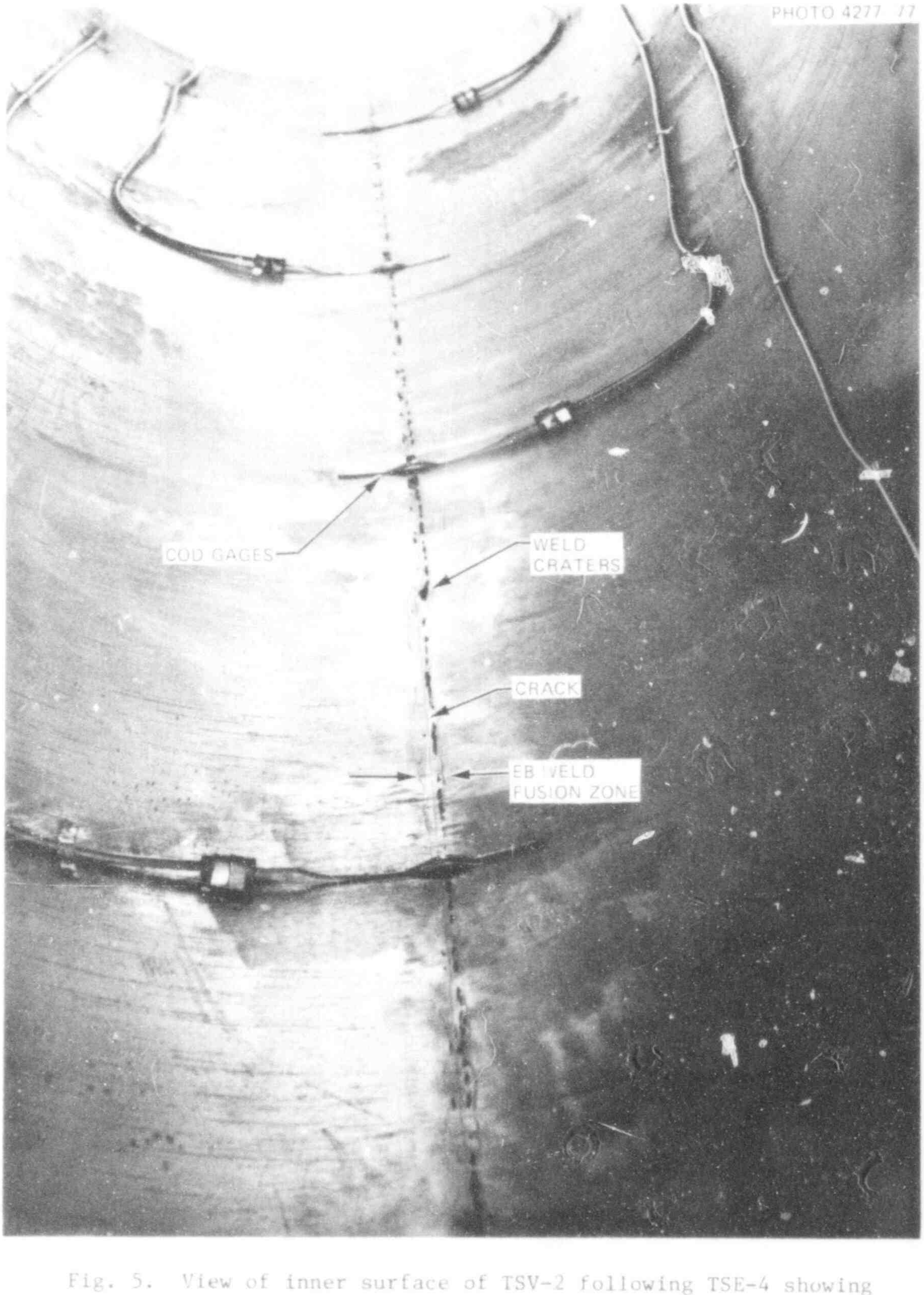

Fig. 5. View of inner surface of TSV-2 following TSE-4 showing electron beam weld flaw and four of five COD gages. Gages buckled during experiment.

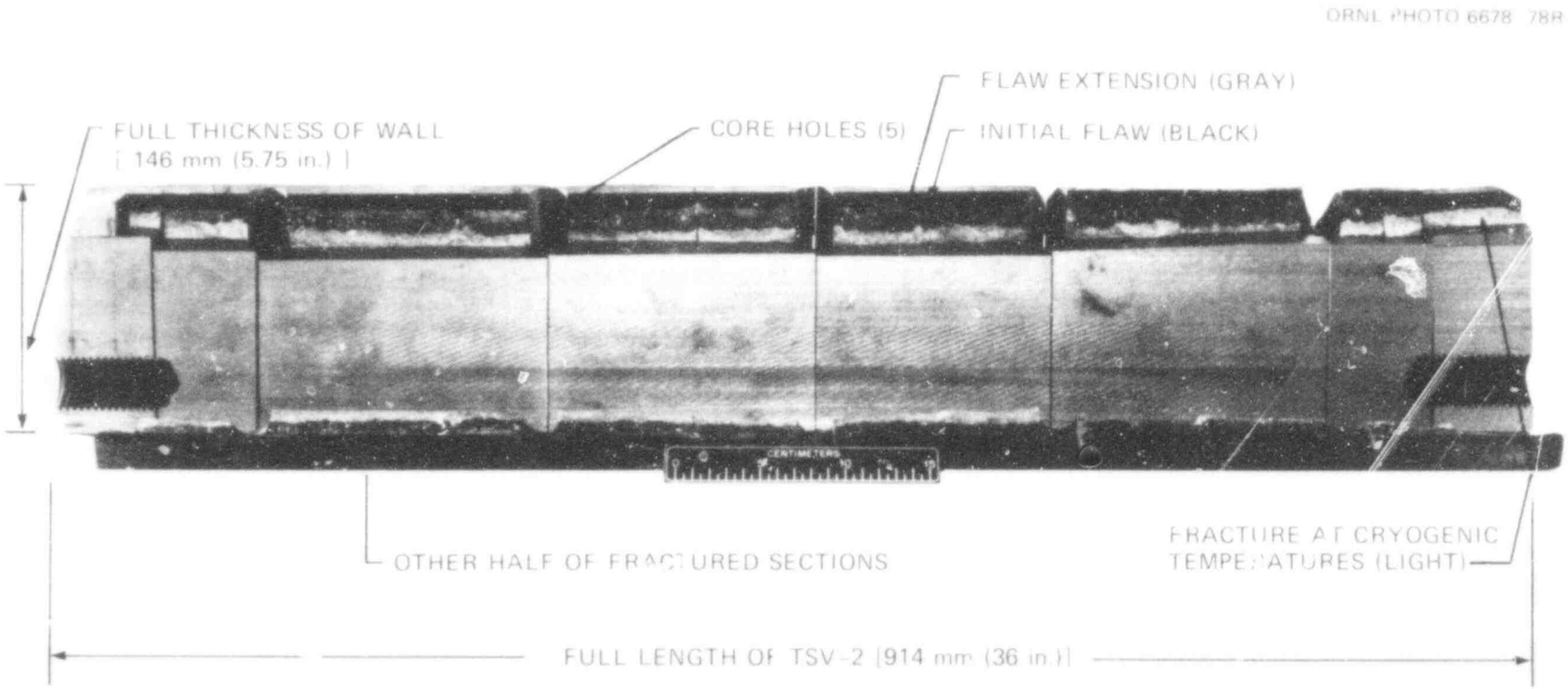

Fig. 6. Section of TSV-2 showing fracture surfaces following TSE-4. Flawed region sectioned as shown before completing fracture at cryogenic temperature. Core holes machined following TSE-4 prior to flaw removal.

to 150 sec, are shown in Fig. 7. Tabulated values of K_I and temperature at 150 sec for the two actual crack depths (depths determined posttest by destructive means) and the corresponding material toughness values are presented in Tables 3 and 4. It is observed in these tables that the nominal calculated value of K_I corresponding to crack initiation (114 MN $m^{-3/2}$) and the average value of K_{Ic} taken from Fig. 4 (108 MN $m^{-3/2}$) agree within 6%, which is well within the uncertainty in both numbers. The static K_I value corresponding to crack arrest (127 MN $m^{-3/2}$ at 131°C) is 11% greater than that corresponding to crack initiation (114 MN $m^{-3/2}$ at 77°C).

Table 3. TSE-4 initiation and arrest data

Event	Crack depth (mm)	Temperature (°C)	ORNL static analyses, K_I[a] (MN $m^{-3/2}$)	BCL analyses, K_I (MN $m^{-3/2}$)
Initiation	11 ± 1	77 ± 3	114 ± 2	112 ± 11[b]
Arrest	23 ± 2	131 ± 9	127 ± 1	124 ± 15[c]

[a]Variation associated with uncertainty in crack depth; does not include uncertainty in K_I calculation, which is ∿±10%.

[b]Static.

[c]Dynamic.

Table 4. TSV-1 and TSV-2 toughness data

Event	Temperature (°C)	K_{Ic}[a] (MN $m^{-3/2}$)	K_{ID} (MN $m^{-3/2}$)	K_{Ia} (MN $m^{-3/2}$)
Initiation	77[b]	108 ± 3	153 ± 15	103 ± 12
Arrest	131[b]	158 ± 10	173 ± 20	123 ± 15

[a]Variation associated with uncertainty in crack depth in TSV-2, and thus temperature. Uncertainty in K_{Ic} data (Fig. 4) is ∿ 20%.

[b]K_{ID} and K_{Ia} measurements were performed at 78 and 126°C, respectively (BCL data).

ORNL-DWG 79-4355R ETD

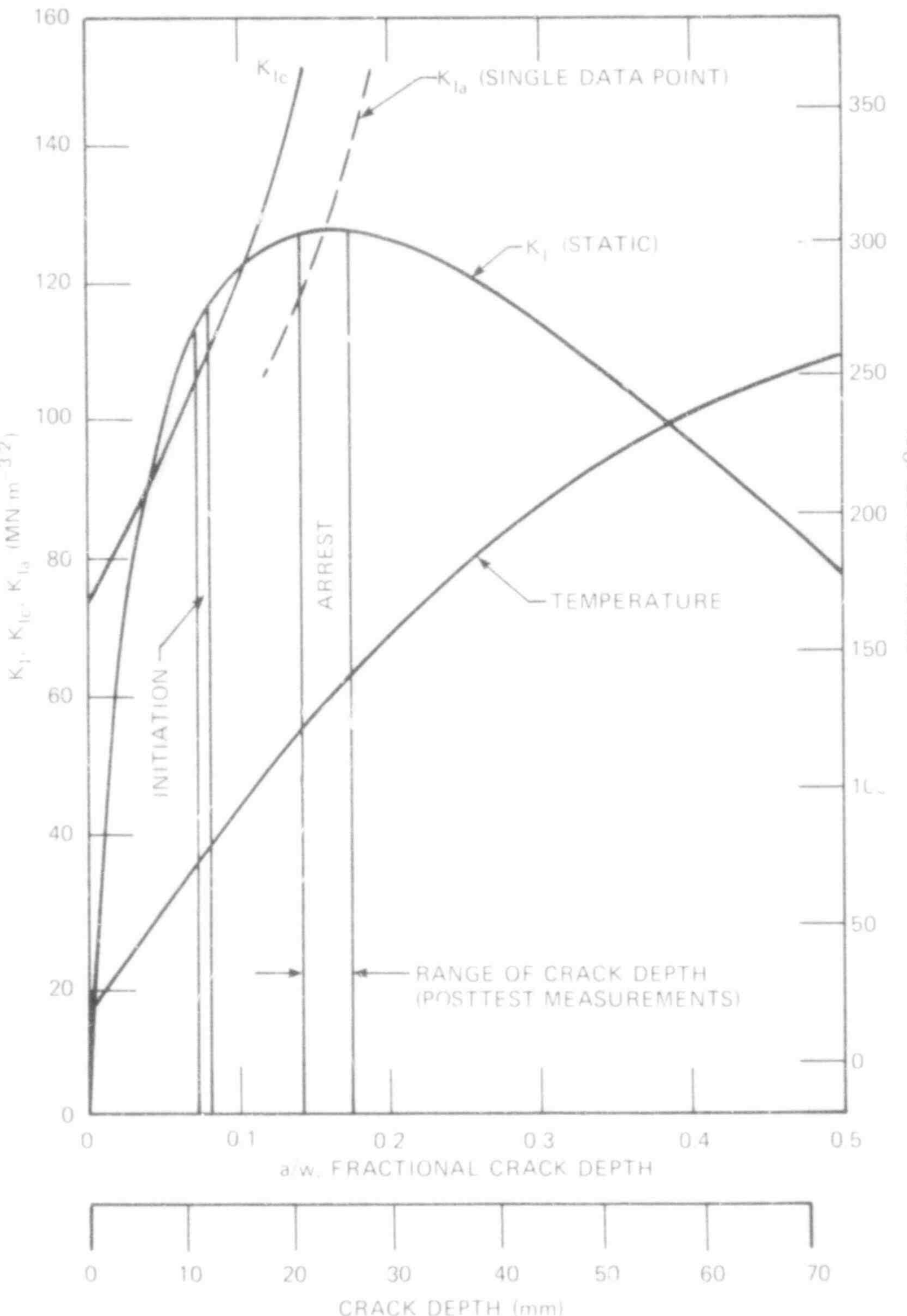

Fig. 7. Measured radial temperature distribution and corresponding calculated K_I distribution at 150 sec in TSE-4 transient. Initiation and arrest events are indicated.

5. ANALYSIS OF TSE-4

5.1 ORNL Static Analysis

A static interpretation of the TSE-4 initiation-arrest event is displayed graphically in Fig. 8, which is a plot of fractional crack depth (a/w) corresponding to $K_I = K_{Ic}$, $K_I = K_{Ia}$, and $(K_I)_{max}$* vs time in the transient. This plot is constructed using the $(K_I)_{max}$ value and the intersections of the K_{Ic} and K_{Ia} curves with the K_I curve (as shown in Fig. 7) for different times in the transient. A brief study of Fig. 8 is useful in helping to determine whether the initial flaw was sharp and to determine

---

*$dK_I/dt = 0$.

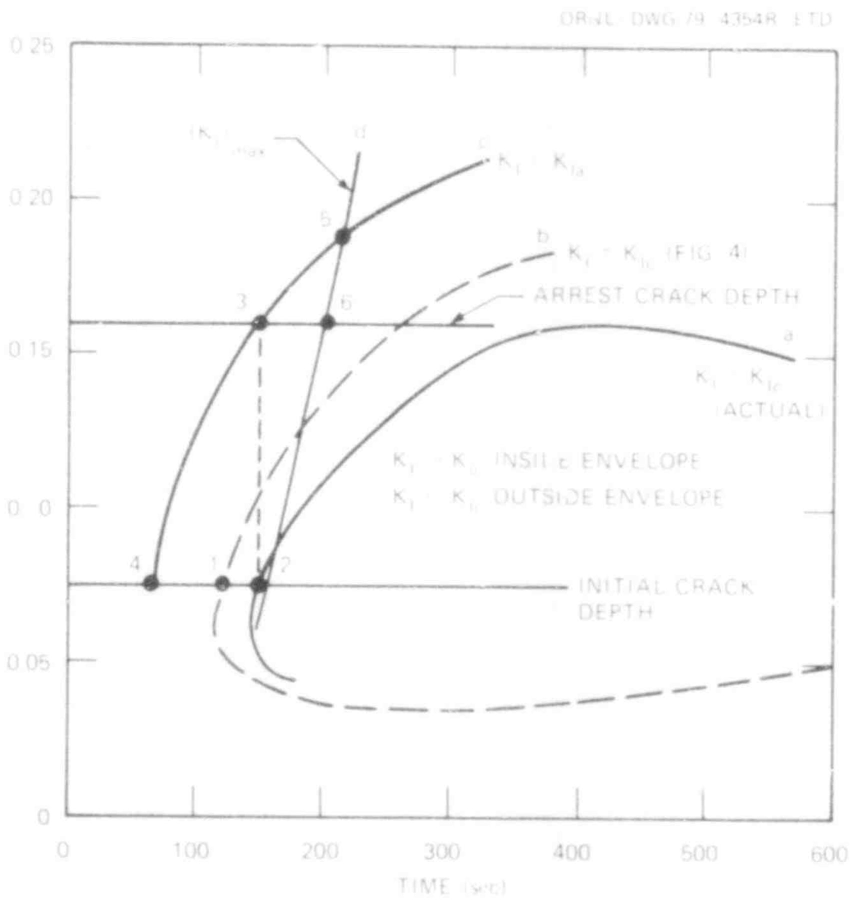

Fig. 8. Fractional crack depth corresponding to $K_I = K_{Ic}$, $K_I = K_{Ia}$, and $(K_I)_{max}$ vs time in transient for TSE-4.

508 026

the relationship between K_{Ic} and K_{Im}. (It will be shown later in this report that, for TSE-4, $K_{Im} \cong K_{Ia}$).

Curve b in Fig. 8 is based on the best pre-TSE-4 estimate of the K_{Ic} vs temperature curve (K_{Ic} curve in Fig. 4), while curve a is based on the actual results of TSE-4; that is, at the time of initiation (and for the corresponding temperature), $K_{Ic} = K_I$(calculated), and it was assumed that for all other temperatures, K_{Ic}(actual) = K_{Ic}(Fig. 4) [K_{Ic}(actual)/ K_{Ic}(Fig. 4)]$_{initiation}$. In both cases, it was assumed that the initial flaw was sharp; the validity of this assumption was confirmed by photomicrographs of test flaws prepared in an identical manner and by the observed crack behavior, as discussed below. If in actuality the TSE-4 flaw were blunt, a curve to the left of curve a, such as curve b, would be appropriate. In this event, the time of initiation would be delayed from point 1 to point 2, the actual time of initiation, and the K_{Ic} values would be somewhat less than those corresponding to curve a. An extreme in this regard would be for $K_{Ic} = K_{Ia}$ (or K_{Im}), in which case the initial flaw would have to be sufficiently blunt to delay the time of initiation from point 4 to point 2.

The crack jump that occurred in TSE-4 is represented by the vertical distance from point 2 to point 3 in Fig. 8, and this particular event is not inconsistent with the crack being either sharp or blunt. However, if $K_{Ic} = K_{Ia}$, the crack would have continued to propagate along curve c, after having arrested at point 3, until curve d was intercepted at point 5. Instrumentation used to detect crack initiation and arrest gave no indication that this happened. If the initial flaw were blunt to the extent that the $K_I = K_{Ic}$ curve passed between points 3 and 6 ($K_{Ia} < K_{Ic}$), there would be a delay following the arrest event (3) and then a second initiation-arrest event, but no such event was detected. These are further indications that the initial flaw was sharp.

If the $K_I = K_{Ic}$ curve passed to the right of point 6, presumably reinitiation would not take place, even though $K_I > K_{Ic}$ after point 6, because K_I would be decreasing with time;[15] also, perhaps $(K_I/K_{Ic})_{max}$ would be less than unity for the arrest crack depth, which, as indicated, may have been the actual situation.

In conclusion, analysis of data from TSE-4 indicates that the $K_I = K_{Ic}$ curve does not pass between points 3 and 6, implying that $K_{Ia} < K_{Ic}$. On the other hand, the analysis and the uncertainty in the K_{Ic} vs temperature data (Fig. 4) allow the curve to lie anywhere between point 6 and curve a. However, observed crack behavior and photomicrographs of test flaws indicate that the initial flaw was sharp. Furthermore, the K_{Ic} values used to obtain curve a are only 6% above the average K_{Ic} curve in Fig. 4. Thus all the data are consistent with the initial crack being sharp, with curve a as the correct $K_I = K_{Ic}$ curve in Fig. 8, and with $K_{Ia} < K_{Ic}$.

5.2 BCL Dynamic Analysis

Two dynamic calculations pertaining to TSE-4 were made by BCL and are reported in Ref. 16. For both cases, the initial crack depth and the stress-intensity factor at the time of initiation (K_Q) were taken to be 11 mm and 112 MN $m^{-3/2}$,* respectively; it was assumed that $K_{ID} \neq f(\dot{a})$, and thus $K_{Im} = K_{ID}$. For the first calculation and as a first approximation, it was further assumed that K_{Im} was only slightly less than K_{Ic} at the initiation temperature, and the K_{Im} vs temperature curve was approximated by the linear relation identified as Case I in Fig. 9. Results of this calculation indicated a 6-mm crack jump compared to the actual jump of 12 mm; the dynamic stress-intensity factor at the instant of arrest was nearly equal to the static value, indicating that dynamic effects for a 6-mm crack jump in TSE-4 were small.

The calculated crack jump can be increased by decreasing K_{Im}; thus for the second calculation, the K_{Im} curve in Fig. 9 (Case I) was shifted to the right an arbitrary amount (~58°C). This K_{Im} vs temperature curve is referred to as Case II in Fig. 9. The result of this calculation was a crack jump of 19 mm. Once again, the dynamic stress-intensity factor at the instant of arrest was nearly equal to the static value, indicating small dynamic effects for the 19-mm jump as well.

The results of these two calculations show that the actual crack jump of 12 mm had essentially no dynamic effect associated with it, and, thus,

*Calculated by BCL for K_I(static) at initiation.

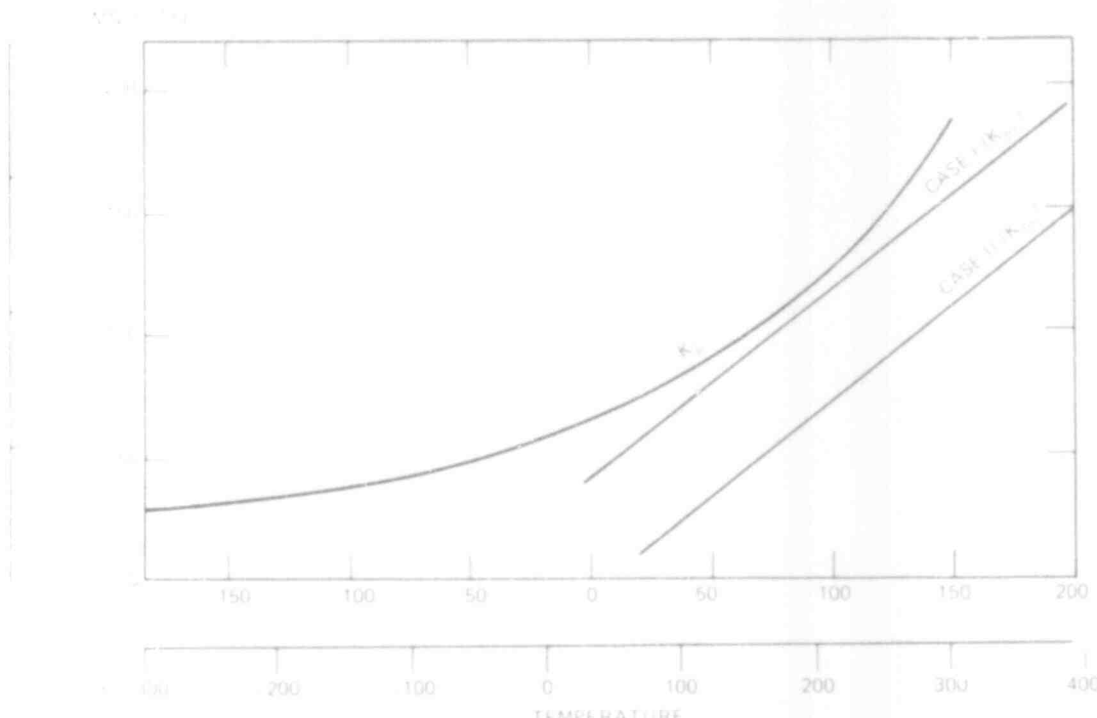

Fig. 9. K_{Ic} vs temperature from Fig. 4 and K_{Im} vs temperature curves by BCL in dynamic analysis of TSE-4.

[illegible] be nearly equal to the static arrest toughness (K_{Ia}) calculated [illegible]. For the given set of assumptions mentioned above, the value of [illegible] at [illegible]°C required for a dynamically calculated crack jump of 12 mm is [illegible] MN $m^{-3/2}$ (determined by interpolation),[17] which agrees very well with [illegible] static value (127 MN $m^{-3/2}$). The small difference that does exist is attributed to differences in the two codes (ORNL finite element and BCL finite difference) used to make the two calculations, as indicated by a comparison of the calculated K_I values at initiation (Table 3).

508 029

6. DISCUSSION AND CONCLUSIONS

The application of the particular dynamic method of analysis to TSE-4 indicates that the run-arrest event in TSE-4 was essentially void of dynamic effects at arrest. Thus the stress-intensity factors at arrest calculated using the static and dynamic models should and do agree; furthermore, this stress-intensity factor can be interpreted as K_{Im}, the crack-arrest toughness of the cylinder material. The particular value obtained ($\sim$127 MN $m^{-3/2}$) is associated with a temperature of 131°C and is 24% less than the K_{Ic} value deduced from TSE-4 for the same temperature.

A precise value of K_{Im} was not determined from the laboratory testing of the DCB specimens because of insufficient data; this prevented a comparison of K_{Im} values obtained from DCB specimens and deduced from TSE-4. However, it is possible and of interest to compare the latter value with K_{Ia} measured with the DCB specimens. The K_{Im} value deduced from TSE-4 at 131°C was 124 MN $m^{-3/2}$, and the DCB K_{Ia} value corrected to the same temperature was 127 MN $m^{-3/2}$, both obtained using the same BCL method of analysis.

Certainly all of the preceding analyses are subject to the effects of uncertainties in the calculations and experimental data. The most probable values were used in the analyses, and no attempt was made to conduct a sensitivity analysis. (The estimated uncertainties pertaining to the initiation and arrest events in TSE-4 and to the DCB data are included in Tables 3 and 4.) It is important to note, however, that no significant anomalies were encountered in the application of the dynamic method of analysis to either the DCB specimens or TSE-4.

508 030

REFERENCES

1. R. D. Cheverton, S. K. Iskander, and S. E. Bolt, *Applicability of LEFM to the Analysis of PWR Vessels Under LOCA-ECC Thermal Shock Conditions*, ORNL/NUREG-40 (October 1978).

2. R. D. Cheverton and S. E. Bolt, *Pressure Vessel Fracture Studies Pertaining to a PWR LOCA-ECC Thermal Shock: Experiments TSE-3 and TSE-4 and Update of TSE-1 and TSE-2 Analysis*, ORNL/NUREG-22 (December 1977).

3. R. D. Cheverton, *Pressure Vessel Fracture Studies Pertaining to a PWR LOCA-ECC Thermal Shock: Experiments TSE-1 and TSE-2*, ORNL/NUREG/TM-31 (September 1976).

4. G. T. Hahn et al., *Critical Experiments, Measurements, and Analysis to Establish a Crack Arrest Methodology for Nuclear Pressure Vessel Steels*, Third Annual Progress Report, October 1976–September 1977, NUREG/CR-0057, BMI-1995 (May 1978).

5. M. F. Kanninen, C. Popelar, and P. C. Gehlen, "Dynamic Analysis of Crack Propagation and Arrest in the Double-Cantilever-Beam Specimens," *Fast Fracture and Crack Arrest*, ASTM-STP 627, pp. 19–38, July 1977.

6. R. G. Hoagland et al., "A Crack Arrest Measuring Procedure for K_{Im}, K_{ID}, and K_{Ia} Properties," *Fast Fracture and Crack Arrest*, ASTM-STP 627, pp. 177–202, July 1977.

7. G. R. Irwin, "Comments on Dynamic Fracturing," *Fast Fracture and Crack Arrest*, ASME-STP 627, pp. 7–18, July 1977.

8. G. T. Hahn et al., *Dynamic Crack Propagation*, G. C. Sih, ed., Lehigh University, Bethlehem, Pa., July 1972, Noordhoff International Publishing, Leyden, The Netherlands, Part VII, pp. 649–62.

9. G. T. Hahn et al., *Proceedings*, Second International Conference on Pressure Vessel Technology, San Antonio, Tex., American Society of Mechanical Engineers, pp. 981–94, October 1973.

10. G. T. Hahn et al., "Fast Fracture Resistance and Crack Arrest in Structural Steels," SSC-Progress Report on Project SR-201, Battelle Columbus Laboratories, Columbus, Ohio (1973).

11. J. K. Kalthoff, J. Beinert, and S. Winkler, "Measurements of Dynamic Stress Intensity Factors for Fast Running and Arresting Cracks in Double-Cantilever-Beam Specimens," *Fast Fracture and Crack Arrest*, ASTM-STP 627, pp. 161–76, July 1977.

12. T. Kobayashi and J. W. Dally, "Relation Between Crack Velocity and the Stress Intensity Factor in Birefringent Polymers," *Fast Fracture and Crack Arrest*, ASTM-STP 627, pp. 257–73, July 1977.

13. G. T. Hahn, personal communication.

14. P. B. Crosley and E. J. Ripling, "Towards Development of a Standard Test for Measuring K_{Ia}," *Fast Fracture and Crack Arrest*, ASME-STP 627, pp. 372–91, July 1977.

508 031

15. F. J. Loss, R. A. Gray, Jr., and J. R. Hawthorne, *Significance of Warm Prestress to Crack Initiation During Thermal Shock*, NRL/NUREG 8165, Naval Research Laboratory, Washington, D.C. (September 1977).

16. R. G. Hoagland et al., "Analysis of Crack Arrest in Reactor Pressure Vessels," paper presented at the ASME Pressure Vessel and Piping Conference, Montreal, Canada, June 1978.

17. G. T. Hahn, personal communication.

508 032

NUREG/CR-0767
ORNL/NUREG-57
Dist. Category RF

Internal Distribution

1. S. E. Bolt
2. R. H. Bryan
3-23. R. D. Cheverton
24. J. M. Corum
25. R. F. Hibbs
26. P. P. Holz
27-31. S. K. Iskander
32. J. G. Merkle
33. S. E. Moore
34. F. R. Mynatt
35. H. A. Pohto (Y-12)
36. H. Postma
37. J. L. Rich
38. W. J. Stelzman
39. H. E. Trammell
40. G. D. Whitman
41. Patent Office
42-43. Central Research Library
44. Y-12 Document Reference Section
45-47. Laboratory Records Department
48. Laboratory Records, RC

External Distribution

49. C. Z. Serpan, RSR, Nuclear Regulatory Commission, Washington, D.C. 20555
50. Office of Assistant Manager, Energy Research and Development, DOE, ORO
51-52. Technical Information Center, DOE
53-392. Given distribution under category RF (10—NTIS)

508 033